One-step hydrothermal synthesis of CTAB-modified SiO_2 for removal of bisphenol A

Yefei Zhang, Chao Liu, Lijun Luo, Yingying Shi, Yu Chen, Shan Wang, Longchun Bian and Fengzhi Jiang

ABSTRACT

A stable SiO_2 material marked as CTAB-Ms(x) was synthesized by a novel sol-gel method. It was modified with hexadecyl trimethyl ammonium bromide (CTAB), which resulted in high adsorption capacity. Its microstructure and surface functional groups were characterized by scanning electron microscope, transmission electron microscope and Fourier transform infrared. The results showed that CTAB-Ms(x) had a core/shell structure in which the core was a CTAB micelle and the shell was SiO_2. The prepared material was applied to adsorb bisphenol A (BPA). Pseudo-first-order kinetics equation, pseudo-second-order kinetics equation, Langmuir adsorption isotherm model, Temkin adsorption isotherm model, and thermodynamic equations were used to fit and analyze the experiment results. The theoretical maximum adsorption capacities calculated according to linear and non-linear forms of the Langmuir isotherm were 370.37 $mg \cdot g^{-1}$ and 198.80 $mg \cdot g^{-1}$, and the adsorption equilibrium time was 120 min. A mechanism study showed that the high adsorption capacity was attributed to the solubilization effect of the CTAB micelle.

Key words | adsorption, BPA, CTAB, SiO_2

Yefei Zhang
Chao Liu
Yingying Shi
Yu Chen
Shan Wang
Fengzhi Jiang (corresponding author)
School of Chemical Science and Technology,
Yunnan University,
Kunming 650091,
China
E-mail: *fengzhij@ynu.edu.cn*

Lijun Luo
The Engineering Laboratory of Polylactic Acid-Based Functional Materials of Yunnan Province,
School of Chemistry and Biotechnology,
Yunnan MinZu University,
Kunming 650500,
China

Longchun Bian
Advanced Analysis and Measurement Center,
Yunnan University,
Kunming 650091,
China

INTRODUCTION

Endocrine-disrupting chemicals (EDCs) have attracted increasing attention in the last few decades, owing to their potential impacts on aquatic environments. EDCs can cause abnormalities in the functions of endocrine systems of wildlife and humans (Rochester 2013). EDCs represent a broad class of natural and synthetic chemicals, such as bisphenol A (BPA), 17β-estradiol, and 17α-ethynyl estradiol. They have estrogenic activity and they can alter the normal endocrine functions and affect the physiological status of animals and human beings. Owing to its extensive usage in industry as an intermediate for the production of polycarbonate plastics and as a major component of epoxy (Chen *et al.* 2016), BPA has been widely distributed in the water environment during the manufacturing and application processes, and it has been detected in different water resources, soils, aquatic animals, food and human beings in China and abroad. BPA is stable in the environment, hardly degraded and tends to bio-accumulate, which makes it very urgent and important for us to develop a sustainable, effective and economical method to remove BPA in water (Manfo *et al.* 2014).

So far, various technologies have been studied to remove BPA from water systems, such as biodegradation (Balest *et al.* 2008), photochemical catalysis (Zhang *et al.* 2014), and adsorption (Alsbaiee *et al.* 2016). Among those methods, adsorption is a superior and promising method for removing contaminants from the water system in terms of low cost, ease of operation, and lack of harmful secondary products. Several researchers synthesized and used various kinds of adsorbents to remove BPA, such as porous β-cyclodextrin polymer (Alsbaiee *et al.* 2016), hydrophobic Y-type zeolite (Tsai *et al.* 2006), organic–inorganic hybrid mesoporous material (Ph-MS) (Kim *et al.* 2011), clay minerals and zeolites (Dong *et al.* 2010). One trait they all have in common is their adsorption capacity for BPA due to the Brunauer–Emmett–Teller (BET) surface area. So, there will be a sharp decline of the absorption capacity if the BET surface area is reduced. Mesoporous SiO_2 could be conveniently achieved by sol-gel processes (Zhao *et al.* 2000) and could be modified with various functional groups, such as vinyl alcohol (Wu *et al.* 2010) and

doi: 10.2166/wst.2017.272

P123 (Teng *et al.* 2011), and proved to be effective adsorbents for Cu^{2+} and Hg^{2+}, respectively. The main adsorption mechanism was electrostatic interaction. These research studies showed that there was a sharp rise of the absorption capacity after modification. SiO_2 could be modified by cationic surfactants. It is an ideal adsorbent for removing BPA because of its special character, which has been rarely reported.

In this work, hexadecyl trimethyl ammonium bromide (CTAB)-modified silica absorbents with core/shell structure have been prepared by a novel sol-gel method, and marked as CTAB-Ms(x). The obtained CTAB-Ms(x) was characterized and used for removal of BPA. Meanwhile, the effects of experimental conditions on the BPA adsorption capacity of CTAB-Ms(x) were investigated. A possible adsorption mechanism is proposed for the removal of BPA over CTAB-Ms(x) on the basis of the above experimental results.

MATERIALS AND METHODS

Materials and reagents

All chemicals used in experiments were analytical grade, and solutions were prepared with deionized water. The reagents and materials used in this work included CTAB (99%, Aladdin), tetraethyl orthosilicate (Chengdu Kelong Chemical Reagent Co., Ltd), ethanol (Yunnan Shandian Pharmacy Co., Ltd), NaOH (96%, Tianjin Yongda Chemical Reagent Co., Ltd), HCl (36–38%, Chongqing Dongchuan Chemical Co., Ltd), BPA (99%, Sigma-Aldrich) and filter membrane (pore size 0.45 μm, Tianjin Hengao Technology Development Co., Ltd).

Preparation of CTAB-Ms(x)

CTAB-Ms(x) could be simply obtained by a novel sol-gel method. First, 1.65 g of CTAB was dissolved with 70.5 mL of deionized water under stirring at 55 °C. Then, 20 mL of NaOH solution (1 mol·L^{-1}) and 7.3 mL of tetraethyl orthosilicate were added to the above CTAB solution. The reaction mixture was stirred for 48 h to obtain a white gel. The mother liquor was decanted, and the products of white gel were washed alternately with ethanol and deionized water several times until the filtrate became foamless. The product was dried under vacuum at 100 °C for 12 h.

Preparation of Ms (ds)

CTAB-Ms(x) was heated at 550 °C in a muffle furnace for 8 h with a temperature increasing rate of 2 °C·min^{-1}. Then, the white powder was obtained and marked as Ms (ds).

Characterization

Fourier transform infrared (FT-IR) spectra were obtained on a Nicolet iS10 FT-IR spectrometer (Thermo Scientific, Germany). The spectra were obtained using KBr pellets over the wavenumber range of 4,000–400 cm^{-1} with a resolution of 2 cm^{-1}.

The crystal structures of the sample powders were characterized by a TTRIII X-ray diffractometer (XRD, Rigaku, Japan) with Cu Kα radiation in the 2θ range from 10° to 80°. The scanning rate was 10°/min and the step size was 0.02°/s; the accelerating voltage and the applied current were 40 kV and 200 mA, respectively.

Morphology of the powder materials was examined by scanning electron microscope (SEM) (FEI QUANTA 200) observation at 20 kV. The particle morphology was observed using a transmission electron microscope (TEM) (JEM-2100) operated at 200 kV.

Adsorption equilibrium experiments

Batch experiments were carried out in a shaker incubator (SUKUN SKY-200B). The effects of various adsorption parameters such as contact time, initial concentration of BPA solution, solution temperature and the pH of the solutions on the adsorption process were studied and optimized. In general, sorption experiments were performed by equilibrating 0.01 g of sorbent with 50 mL of the BPA solution in 50 mL conical flasks on a shaker at 200 rpm and 298 K for 6 h. The BPA solution concentration was 20 mg·L^{-1}; the initial pH values, which were measured using a pH meter (DENVER instrument UB-7), were adjusted to 5.8 unless otherwise stated, by adding minimum amounts of HCl solution. At the end of the adsorption, all the suspensions were filtered using cellulose acetate membrane filters with pore diameter of 0.45 μm, and the filtrates were analyzed for total BPA. The concentration of the BPA solution was determined using a UV/visible spectrophotometer (UV-2401PC). All experiments were performed in duplicate and the average values were recorded. The amounts of the BPA at

equilibrium q_e ($mg \cdot g^{-1}$) on the adsorbent were calculated by Equation (1):

$$q_e = \frac{(C_0 - C_e)\, V}{m} \tag{1}$$

where C_0 ($mg \cdot L^{-1}$) is the initial concentrations of aqueous solution, C_e ($mg \cdot L^{-1}$) is the equilibrium concentration, V (L) is the volume of the solution, and m (g) is the mass of the adsorbent.

Adsorption kinetic study

Adsorption experiments were carried out by mixing 0.01 g of the CTAB-Ms(x) and 50 mL 20 $mg \cdot L^{-1}$ BPA solution at 298 K, on a shaker with rotation speed of 200 rpm. After different time intervals, as adsorption time, of 5, 10, 20, 30, 60, 120 and 360 min, the solids and liquids were separated by filter membrane, and the exact concentration of BPA remaining in the solution was measured by a UV/visible spectrophotometer (UV-2401PC).

Adsorption isotherm study

Adsorption experiments were carried out by mixing 0.01 g of the CTAB-Ms(x) (or Ms (ds)) and BPA solution with initial concentrations of 5, 20, 30, 40 and 80 $mg \cdot L^{-1}$ at 298 K, on a shaker with rotation speed of 200 rpm. In order to reach the saturated adsorption, the adsorption was run for 6 h. When the adsorption finished, the concentrations of the BPA were analyzed.

Adsorption thermodynamic study

The effect of solution temperature on the adsorption process was studied at different temperature of 288, 298, 308 and 318 K with contact time of 6 h by adjusting a temperature-controlled mechanical shaker (SUKUN SKY-200B). The dosage of CTAB-Ms(x) was 0.01 g. In this experiment, the thermodynamic parameters of the adsorption were determined.

Effect of solution pH

In order to study the influence of pH on adsorption, the initial pH of the solutions was varied from 2 to 10. The pH was adjusted by adding 0.1 $mol \cdot L^{-1}$ HCl solutions or 0.1 $mol \cdot L^{-1}$ NaOH solutions and was measured using a pH meter (Denver instrument UB-7). Adsorption was carried out by adding 0.01 g of CTAB-Ms(x) (or Ms (ds)) into 50 mL of 20 $mg \cdot L^{-1}$ BPA solution at 298 K, on a shaker at rotation speed of 200 rpm, and the solid–liquid contact time was 6 h.

Error analysis

The non-linear regression has been an important tool to determine the best isotherm model compared to the experimental data. Due to the inherent bias resulting from linearization, four non-linear error functions were applied to evaluate the best fit into the isotherm models of the experimental equilibrium data. The error equations employed were as follows (Shayesteh *et al.* 2016).

Non-linear chi-square test (χ^2):

$$\chi^2 = \sum_{i=1}^{n} \left[\frac{(q_{e,exp} - q_{e,calc})^2}{q_{e,calc}} \right]_i \tag{2}$$

The average relative error (ARE):

$$\mathrm{ARE} = \sum_{i=1}^{n} \left[\frac{(q_{e,exp} - q_{e,calc})}{q_{e,exp}} \right]_i \tag{3}$$

A derivative of Marquardt's percent standard deviation (MPSD):

$$\mathrm{MPSD} = \sum_{i=1}^{n} \left[\frac{(q_{e,exp} - q_{e,calc})^2}{q_{e,exp}} \right]_i \tag{4}$$

The average percentage errors (APE):

$$\mathrm{APE} = \frac{\sum_{i=1}^{n} [(q_{e,exp} - q_{e,calc})/q_{e,exp}]_i}{\mathrm{N}} \times 100 \tag{5}$$

In the above equations, the subscripts 'exp' and 'calc' indicate the experimental and calculated values of adsorption capacities, respectively, and N is the number of observations in the experimental data.

RESULTS AND DISCUSSION

Adsorbent characterization

FT-IR spectrograms analysis

In order to investigate the chemical compositions of the prepared composites, FT-IR spectroscopy measurements of

commercially purchased CTAB powder, synthesized CTAB-Ms(x) and Ms (ds) were taken as shown in Figure 1(a). For the purchased CTAB powder, the absorption bands at 2,838, 2,923 and 2,993 cm^{-1} were due to -CH_2- bands existing in the CTAB. The absorption bands at 1,080 and 450 cm^{-1} were due to Si-O bands existing in Ms (ds). For the synthesized CTAB-Ms(x) composites shown in Figure 1(a), we found that the -CH_2- bands shifted from 2,838 cm^{-1} to 2,856 cm^{-1} and the peaks of 2,993 cm^{-1} disappeared because of the formation of the bonding between CTAB and part of SiO_2. It was noted that the absorption bands at 1,080 and 450 cm^{-1} were also caused by Si-O bands existing in CTAB-Ms(x). From the above comparison, it may be concluded that CTAB was successfully introduced into SiO_2 for CTAB-Ms(x), and CTAB in Ms (ds) could be completely removed after calcination at 550 °C for 8 h. Figure 1(b) shows the XRD patterns of CTAB-Ms(x) and Ms (ds); the broad peak around 25° is attributed to the amorphous silica (Ge *et al.* 2017).

Morphology

The morphologies of CTAB-Ms(x) and Ms (ds) composites were observed with SEM and TEM as shown in Figure 2. From the SEM images, it can be clearly seen that there was no significant change in the morphology of Ms (ds) powder (Figure 2(b)) compared with CTAB-Ms(x) powder (Figure 2(a)). In order to further investigate the microstructure of prepared particles, CTAB-Ms(x) and Ms (ds) were characterized by TEM as shown in Figure 2(c) and 2(d). It is clear that particles of CTAB-Ms(x) had a core–shell structure. There are many CTAB-cores distributed in the particles of CTAB-Ms(x). The core size was relatively uniform, and the diameter of the CTAB-core was in the range from 10 nm to 50 nm (Figure 2(c)). However, the core–shell structure was completely destroyed after calcination for Ms (ds) as shown in Figure 2(d). The results indicated that the core–shell structure with a silica-shell and CTAB-core had been successfully fabricated in CTAB-Ms(x).

Adsorption of BPA by CTAB-Ms(x)

Adsorption kinetics study

The adsorption amount of BPA along the contact time is shown in Figure 3(a). From Figure 3(a), it can be seen that the adsorption balance can be established in about 120 min for removal of BPA. The adsorbing capacity was 85.58 $mg{\cdot}g^{-1}$ at the equilibrium.

The pseudo-first-order equation and pseudo-second-order equation were used for modeling the kinetics of BPA adsorption. The pseudo-first-order equation (Singh & Tiwari 1997) is generally expressed as Equation (6):

$$\ln(q_e - q_t) = \ln q_e - K_1 t \tag{6}$$

where q_e ($mg{\cdot}g^{-1}$) and q_t ($mg{\cdot}g^{-1}$) are the amounts of BPA adsorbed at the equilibrium and at time t (min), respectively, and K_1 (min^{-1}) is the rate constant of first-order adsorption.

The pseudo-second-order adsorption kinetic rate equation (Ho & McKay 1999) is expressed as Equation (7):

$$\frac{t}{q_t} = \frac{1}{K_2 q_e^2} + \frac{1}{q_e} t \tag{7}$$

where q_e ($mg{\cdot}g^{-1}$) and q_t ($mg{\cdot}g^{-1}$) are the sorption capacity at equilibrium and time t (min), respectively.

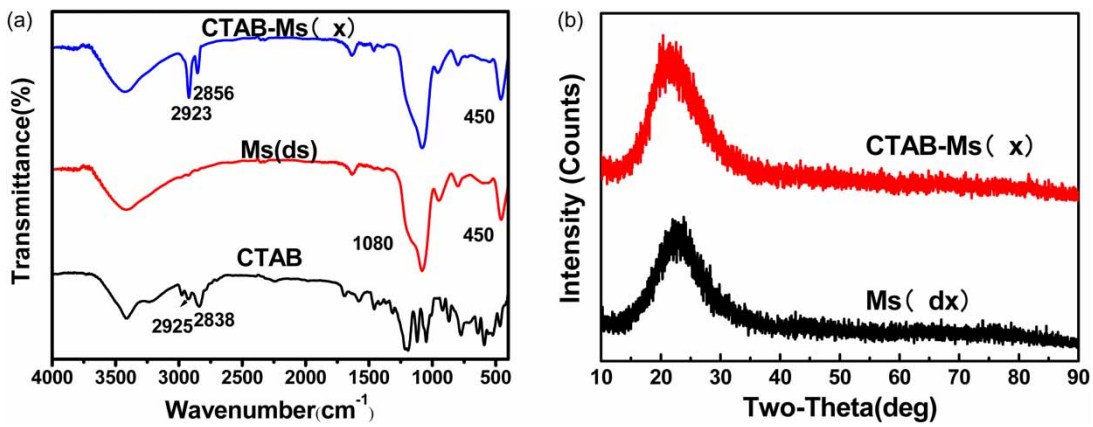

Figure 1 | FT-IR spectra of CTAB-Ms(x), Ms (ds) and CTAB (a); XRD patterns of CTAB-Ms(x), Ms (ds) (b).

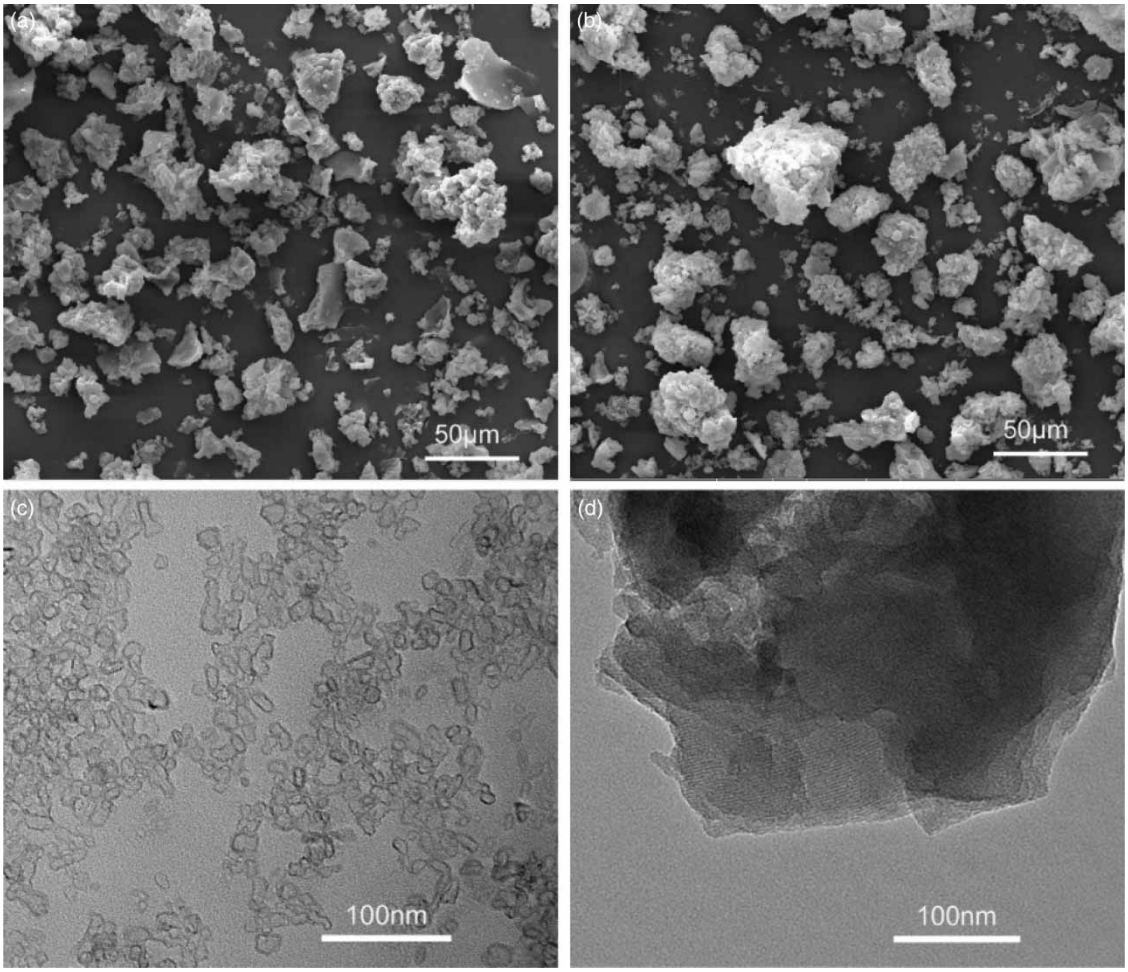

Figure 2 | SEM images of CTAB-Ms(x) (a) and Ms (ds) (b) and TEM images of CTAB-Ms(x) (c) and Ms (ds) (d).

K_2 (g·mg^{-1}·min^{-1}) is the rate constant of the pseudo-second-order sorption.

Figure 3(b) and 3(c) show the result of fitting the experimental data with the linear form of the pseudo-first-order and pseudo-second-order kinetic equations, respectively. In Figure 3(c), a good linear plot of t/q_t versus t was presented and the regression coefficient of it was 0.9998, while the regression coefficient was 0.97005 for the linear plot of $\ln(q_e - q_t)$ versus t (Figure 3(b)). The result confirmed that the pseudo-second-order kinetic model was suitable to describe the adsorption process of BPA on CTAB-Ms(x). Meanwhile, as is shown in Table 1, the difference between the calculated q_e value (86.58 mg·g^{-1}) and the experimental value ($q_e = 85.58$ mg·g^{-1}) was very small, further showing that the adsorption process of BPA on CTAB-Ms(x) could be fitted well with the pseudo-second-order kinetic model, which suggested that the rate-limiting step may be chemisorption (Özacar & Şengil 2003; Coleman *et al.* 2006). In a word, the adsorption of BPA over CTAB-Ms(x) was mainly due to electrostatic interactions between the oxygen atoms of BPA and the CTAB-core (Dong *et al.* 2010).

Adsorption isotherm study

The influence of initial concentration of BPA solution on the adsorbing capacity is shown in Figure 4(a). While the initial concentration of BPA solution increased from 5 to 80 mg·L^{-1}, the adsorbing capacity of CTAB-Ms(x) increased from 22 to 185 mg·g^{-1}, while the adsorbing capacity of Ms (ds) did not increase obviously. When the initial concentration of BPA was less than or equal to 5 mg·L^{-1}, the BPA in the aqueous solution was completely adsorbed by CTAB-Ms(x). The considerable adsorbing capacity could be attributed to the solubilization effect of the CTAB-core. An adsorption isotherm is usually

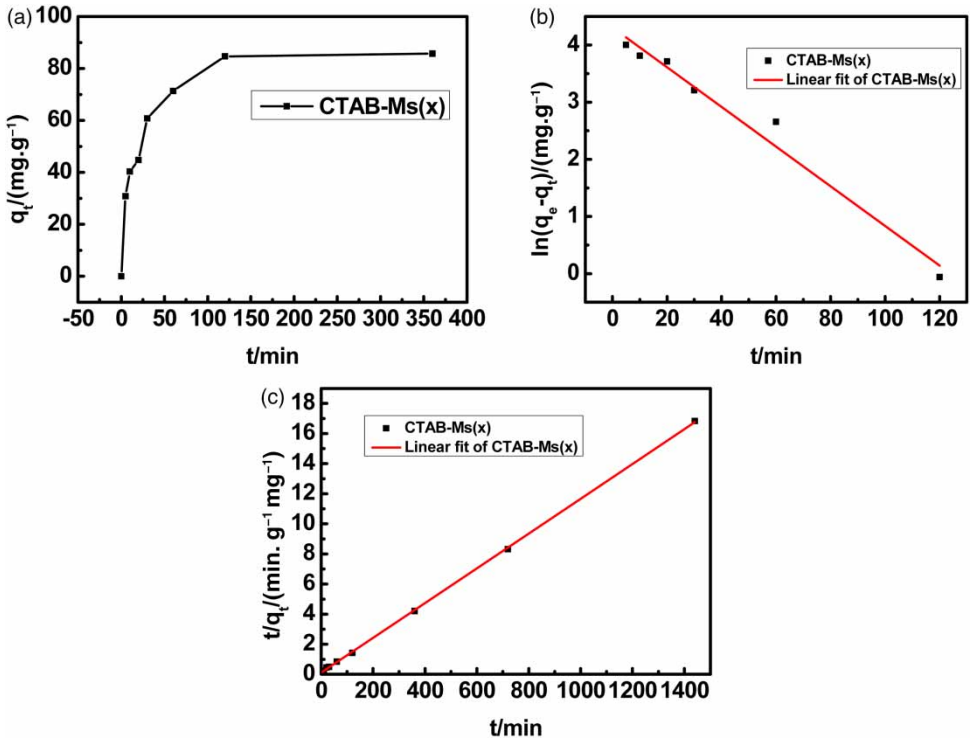

Figure 3 | Experimental variation of adsorbed amounts of BPA on CTAB-Ms(x) versus time (a) and the linear fit of experimental data using pseudo-first-order kinetic model (b) and pseudo-second-order kinetic model (c) ($T = 298$ K; adsorbent dose = 0.2 g·L^{-1}; the initial concentration = 20 mg·L^{-1}; pH value 5.8).

Table 1 | Dynamics parameters for the adsorption of BPA on CTAB-Ms(x) adsorbent

Pseudo-first-order kinetic model				Pseudo-second-order kinetic model			
K_1	R^2	$q_{e.cal}$ (mg·g^{-1})	$q_{e.exp}$ (mg·g^{-1})	K_2	R^2	$q_{e.cal}$ (mg·g^{-1})	$q_{e.exp}$ (mg·g^{-1})
0.0347	0.97005	74.098	85.58	0.0012	0.9998	86.58	85.58

used to describe the adsorption behavior of BPA. Langmuir and Temkin adsorption models are two of the most common types of adsorption isotherm. The Langmuir model has been applied to many sorption processes and used to explain the monolayer adsorption of dyes over a homogeneous surface (Mall *et al.* 2006). The non-linear and linear forms of this model are given by Equations (8-1) and (8-2), respectively:

$$q_e = \frac{q_m k_L C_e}{1 + k_L C_e} \tag{8-1}$$

$$\frac{1}{q_e} = \frac{1}{q_m k_L}\frac{1}{C_e} + \frac{1}{q_m} \tag{8-2}$$

where k_L (L·mg^{-1}) is the Langmuir adsorption constant related to energy of adsorption, q_m (mg·g^{-1}) signifies maximum adsorption capacity, q_e (mg·g^{-1}) is the amount adsorbed at equilibrium concentration C_e (mg·L^{-1}). The constants k_L and q_m were calculated from the slope and intercept of the plot of $1/q_e$ versus $1/C_e$. The values of the constants obtained for the Langmuir isotherm are shown in Table 2.

The Temkin isotherm contains a factor which takes into account the adsorbent–adsorbate interactions. Thus, the equation can be used to describe adsorption on heterogeneous surfaces. By neglecting the lowest and highest concentration values, the model assumes that heat of adsorption (function of temperature) of all molecules in a layer would decrease linearly rather than logarithmically with the increasing surface coverage

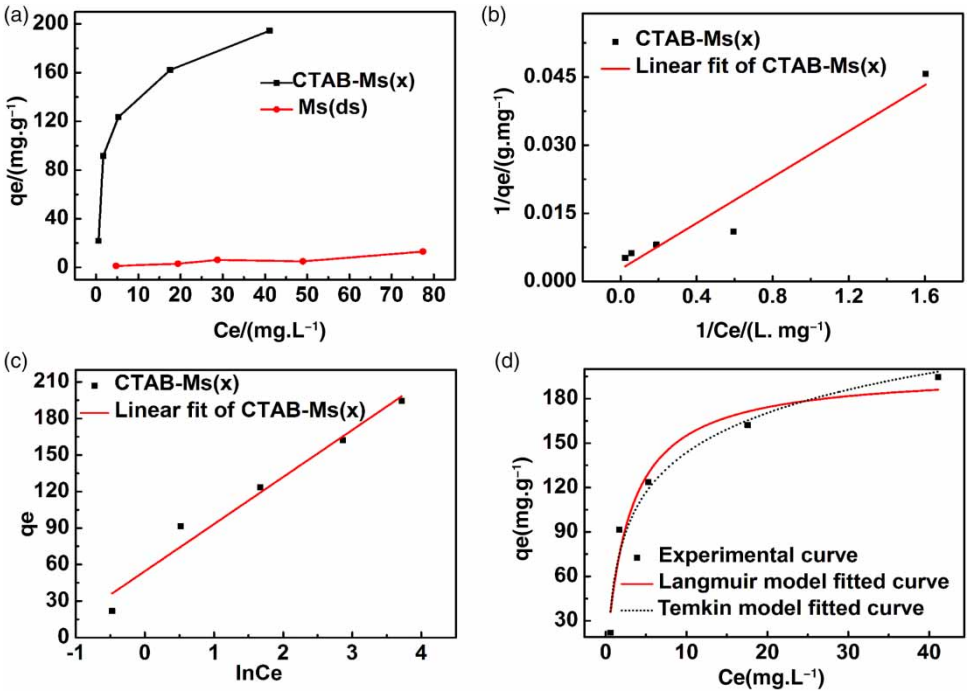

Figure 4 | Effect of the initial concentration on adsorbed BPA (a); linear fitting of experimental data using Langmuir (b) and Temkin (c) sorption isotherms; adsorption isotherms non-linear correlation of BPA adsorption onto the CTAB-Ms(x) using Langmuir and Temkin (d) ($T = 298$ K; adsorbent dose = 0.2 g·L^{-1}; pH value 5.8; time = 360 min).

Table 2 | Adsorption isotherm constants and values of different error analyses for isotherm models (linear and non-linear methods)

	Langmuir equation			Temkin equation	
	Linear	Non-linear		Linear	Non-linear
q_m (mg·g^{-1})	370.37	198.80	b_T (J·mol^{-1})	64.0951	64.0951
K_L (L·mg^{-1})	0.107	0.354	K_T (L·g^{-1})	4.10549	4.10549
R^2	0.9320	0.9481	R^2	0.9697	0.9597
χ^2	86.97	10.74	χ^2	9.8595	9.8596
ARE	−0.7916	−0.5155	ARE	−0.4776	−0.4776
MPSD	112.1	13.53	MPSD	12.927	12.928
APE	−15.83	−10.31	APE	−9.5518	−9.5519

(Huang *et al.* 2010). The non-linear and linear forms of this model are given by Equations (9-1) and (9-2) respectively:

$$q_e = \frac{RT}{b_T} \ln (K_T\, C_e) \tag{9-1}$$

$$q_e = \frac{RT}{b_T} \ln K_T + \frac{RT}{b_T} \ln C_e \tag{9-2}$$

where K_T denotes the equilibrium binding constant (L·g^{-1}), b_T is the constant related to the heat of adsorption (J·mol^{-1}), R is the universal gas constant (8.314 J·mol^{-1}·K^{-1}), and T is the temperature (K). The values of the constants obtained for the Temkin isotherm are also shown in Table 2.

The experimental data were fitted using Langmuir and Temkin isotherm models and the linear and non-linear relationships are shown in Figure 4(b)–4(d), respectively. The values of the Langmuir and Temkin isotherm parameters calculated from adsorption equilibrium data are

listed in Table 2. The high value of the linear and non-linear regression coefficient (R^2) for the Langmuir and Temkin isotherms for CTAB-Ms(x), respectively, shows that these models give good fit to the adsorption isotherm. Meanwhile, the maximum adsorption capacity q_m for the adsorption of BPA on CTAB-Ms(x) were 370.37 mg·g^{-1} (linear) and 198.80 mg g^{-1} (non-linear), respectively. However, the adsorption capacity q_e was only 1.2–16.7 mg·g^{-1} for Ms (ds) (Figure 4(a)). The results indicated that the adsorption of CTAB-Ms(x) depended strongly on its CTAB-core. The adsorption capability of CTAB-Ms(x) and other adsorbents is listed in Table 3. From Table 3, the efficiency for CTAB-Ms(x) removing BPA from aqueous solution was significantly high comparing to other reported absorbents. Unlike most of the other reported adsorbents, the extremely high adsorption capability of CTAB-Ms(x) was attributed to the solubilization of the CTAB-core rather than the high BET surface area. Actually, the BET surface area of CTAB-Ms(x) was too low to be measured.

Adsorption thermodynamics

The effect of temperature on the adsorption of BPA was studied. It was found that the adsorption amount q_e (mg·g^{-1}) decreased while increasing the solution temperature from 298 to 318 K (Figure 5(a)). K_c is the standard thermodynamic equilibrium constant. Thermodynamic parameters, including standard Gibbs free energy change (ΔG^0), standard enthalpy change (ΔH^0), and standard entropy change (ΔS^0) (Yurtsever & Sengil 2009), are calculated using the following Equations (10)–(13):

$$K_c = \frac{C_a}{C_e} \tag{10}$$

$$\Delta G^0 = \Delta H^0 - T\Delta S^0 \tag{11}$$

$$\Delta G^0 = -R\,T\,\ln K_c \tag{12}$$

Table 3 | Comparison of adsorption capacity for BPA with other reported absorbents

Adsorbent	pH	T (K)	S_{BET} ($m^2 \cdot g^{-1}$)	q_m[a] (mg·g^{-1})	ref
CTAB-Ms(x)	NA[b]	298	–	370.37 (Linear) 198.80 (Non-linear)	Our study
Vinyl–SiO_2	NA[b]	298	–	136.97	Zhou *et al.* (2013)
Modified CNTs	6.0	280.15	95	70	Kuo (2009)
SMZFA F prepared from coal fly ash	10.4	298	91.5	114.9	Dong *et al.* (2010)
SMZFA L prepared from coal fly ash	9.6	298	50.6	56.8	Dong *et al.* (2010)
Hydrophobic Y-type zeolite	7.0	298	504	111.1	Tsai *et al.* (2006)
Ph-MS	NA[b]	298	750	337	Kim *et al.* (2011)

[a]The maximum adsorption capacity calculated by Langmuir adsorption isotherm model.
[b]The pH value is close to natural conditions.

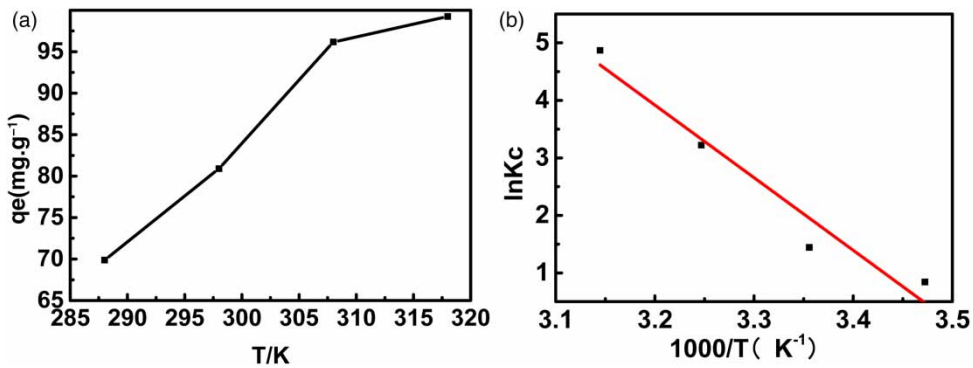

Figure 5 | Effect of the temperature on adsorbed BPA (a) and sorption isotherm (b) (adsorbent dose = 0.2 g·L^{-1}; initial concentration = 20 mg·L^{-1}; pH value 5.8; time = 360 min).

$$\ln K_c = -\frac{\Delta H^0}{RT} + \frac{\Delta S^0}{R} \quad (13)$$

where R (8.314 J·mol^{-1}·K^{-1}) is the gas constant, T (K) is absolute temperature, C_a (mg·L^{-1}) is the change in the concentration of BPA before and after adsorption and, C_e (mg·L^{-1}) is the equilibrium concentration of BPA in the solution.

The linear plots of lnK_c versus 1,000/T are shown in Figure 5(b). From the slope and intercept of this linear plot, the thermodynamic parameters are calculated and listed in Table 4. The positive value of ΔS^0 (384.6 J·mol^{-1}·K^{-1}) suggested the increased randomness of the solution interface during the adsorption of BPA on the adsorbent. The values of ΔG^0 were negative from 288 K to 318 K (−2.015, −3.575, −8.250 and −13.279 KJ·mol^{-1} at 288, 298, 308 and 318 K, respectively). It indicated the process of BPA adsorption by the CTAB-Ms(x) was non-spontaneous from 288 K to 318 K. The positive ΔH^0 value (109.8 KJ·mol^{-1}) indicated that the adsorption of BPA molecules onto CTAB-Ms(x) adsorbent was an endothermic process. The results further explained the fact that the adsorption quantity increased with temperature rising. Moreover, the absolute value of ΔH^0 greater than 60 KJ·mol^{-1} demonstrated that the adsorption process of BPA over CTAB-Ms(x) possess the characteristic of chemisorption since the absolute values of the adsorption heat are Van der Waals force 4–10 KJ·mol^{-1}, hydrophobic interaction 5 KJ·mol^{-1}, hydrogen bond 2–40 KJ·mol^{-1} and chemisorption 60 KJ·mol^{-1} (Sun *et al.* 2010).

Adsorption mechanism

The obtained experimental results are directly associated with the mechanism of the process. The above experiment results showed that CTAB-Ms(x) had a much higher BPA adsorption capability than Ms (ds). In TEM measurements, the completely different morphology between particles of CTAB-Ms(x) and Ms (ds) suggested that the CTAB-core was an important part of the CTAB-Ms(x) adsorbent. Meanwhile, the adsorption kinetics study and adsorption thermodynamics showed that the adsorption of BPA on CTAB-Ms(x) was a chemisorption process. This was further confirmed by the pH effect experiments.

The effect of pH value on the adsorption uptake over different adsorption materials is shown in Figure 6. The initial BPA concentration was 20 mg·L^{-1}, and the amounts of CTAB-Ms(x) and Ms (ds) were 0.2 g·L^{-1}. As shown in Figure 6, the removal capacity of BPA was highly dependent on the pH value of BPA solutions and the adsorption uptake increased from 26 to 95 mg·g^{-1} for CTAB-Ms(x) with pH changing from 2 to 10. Since, as a cationic surfactant, CTAB can easily generate a form of cationic micelle, the deprotonation of BPA makes –OH transform into –O$^-$ (Dong *et al.* 2010) in alkaline environment and it can be easily adsorbed by silicon material with the cationic CTAB-core after CTAB modification; thus the adsorption in alkaline environment was better than that in acid environment (Li *et al.* 2014). The possible reactions in the adsorption process of BPA are shown in Figure 7. Comparing to the high adsorption uptake of CTAB-Ms(x), the adsorption property of Ms (ds) was only about 6 mg·g^{-1} in the pH range of 2 to 10, with no significant change in different pH values. The results revealed that the CTAB-core plays an irreplaceable role in this material. Meanwhile, the solubilization effect of CTAB for BPA endows CTAB-Ms(x) with splendid adsorption performance. In a word, the adsorption of BPA over CTAB-Ms(x) was mainly due to electrostatic interactions between negatively charged –O$^-$ and the cationic micelle, which were very sensitive to the pH value of the solution.

Table 4 | Thermodynamic parameters for the adsorption of BPA on CTAB-Ms(x)

Absorbent	T(K)	ΔG^0 (KJ·mol^{-1})	ΔH^0 (KJ·mol^{-1})	ΔS^0 (J·mol^{-1}·K^{-1})	R^2
CTAB-Ms(x)	288	−2.015	109.8	384.6	0.9301
	298	−3.575			
	308	−8.250			
	318	−13.279			

The cost of BPA removal

The cost of materials and instruments as shown in Table 5. We obtained CTAB-Ms(x) adsorbent by the novel sol-gel

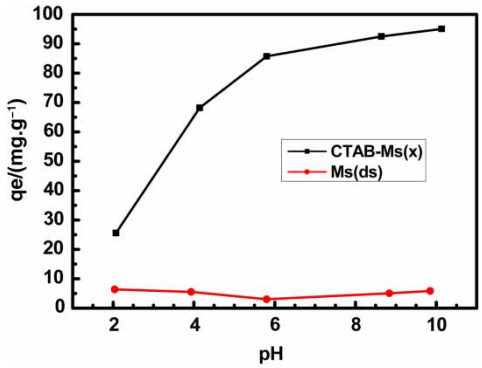

Figure 6 | Effect of pH on adsorption of BPA by CTAB-Ms(x) and Ms (ds) (T = 298 K; adsorbent dose = 0.2 g·L^{-1}; initial concentration = 20 mg·L^{-1}; time = 360 min).

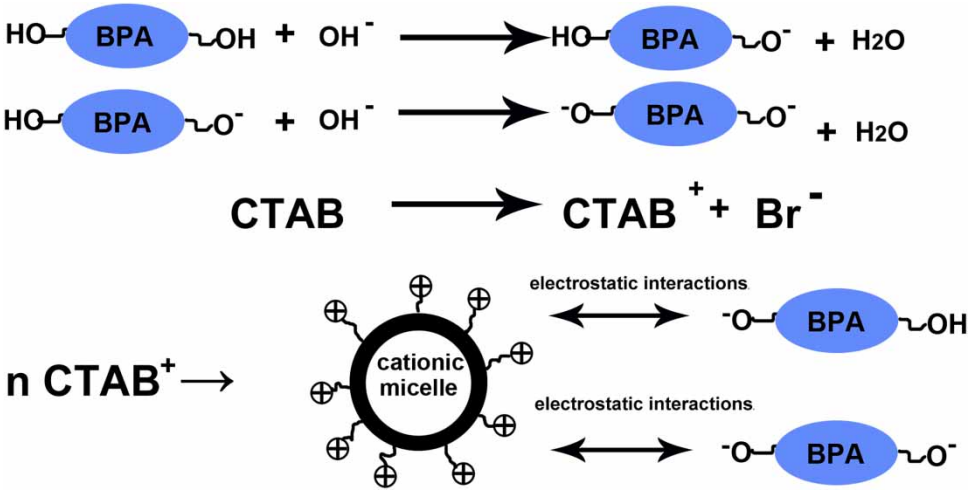

Figure 7 | Scheme of the possible reactions in the adsorption process of BPA.

Table 5 | Cost of materials and instruments

	CTAB	Ethanol	NaOH	Tetraethyl orthosilicate	Shaker incubator
Parameter	100 g	500 mL	500 g	500 mL	580 W
Cost	US$24	US$2	US$2.6	US$33	US$0.244 (6 h)

method and the weight of CTAB-Ms(x) was 1.6 g. The cost of CTAB-Ms(x) was about US$1.8 g^{-1}. From Figure 3(a), it can be seen that the adsorbing capacity of CTAB-Ms(x) for BPA was 85.58 $mg{\cdot}g^{-1}$ at the equilibrium. Consideration of costs shows that CTAB-Ms(x) adsorbent can be used to remove BPA from water at a cost of about US$21.2 g^{-1} without regeneration.

CONCLUSIONS

In this paper, a core–shell structured silica adsorbent marked as CTAB-Ms(x) was synthesized by a novel sol-gel method and was characterized by SEM, TEM and FT-IR techniques. The adsorption process of BPA over CTAB-Ms(x) was investigated in detail. The results indicated that the CTAB-core of CTAB-Ms(x) played a dominant role in enhancing the adsorption capacity of the adsorbent for the BPA removal. The adsorption process was studied with the pseudo-second-order kinetics model, Langmuir adsorption isotherm model and thermodynamic model. The results of the mechanism study illustrated the absorption of BPA on CTAB-Ms(x) was electrostatic interaction. Also, the maximum adsorption capacities calculated according to linear and non-linear forms of the Langmuir isotherm were 370.37 $mg{\cdot}g^{-1}$ and 198.80 $mg{\cdot}g^{-1}$, respectively. CTAB-Ms(x) can be a promising absorbent to remove BPA and other organic pollutants.

ACKNOWLEDGEMENTS

This work was jointly supported by the National Natural Science Foundation of China (No. 21163023 and No. 21261026) and the Key Program of Yunnan Province Foundation (No. 2013FA005).

REFERENCES

Alsbaiee, A., Smith, B. J., Xiao, L., Ling, Y., Helbling, D. E. & Dichtel, W. R. 2016 Rapid removal of organic micropollutants from water by a porous beta-cyclodextrin polymer. *Nature* **529** (7585), 190–194.

Balest, L., Mascolo, G., Di Iaconi, C. & Lopez, A. 2008 Removal of endocrine disrupter compounds from municipal wastewater by an innovative biological technology. *Water Science and Technology* **58** (4), 953–956.

Chen, W.-Y., Shen, Y.-P. & Chen, S.-C. 2016 Assessing bisphenol A (BPA) exposure risk from long-term dietary intakes in Taiwan. *Science of the Total Environment* **543**, 140–146.

Coleman, N. J., Brassington, D. S., Raza, A. & Mendham, A. P. 2006 Sorption of Co^{2+} and Sr^{2+} by waste-derived 11 Å tobermorite. *Waste Management* **26** (3), 260–267.

Dong, Y., Wu, D., Chen, X. & Lin, Y. 2010 Adsorption of bisphenol A from water by surfactant-modified zeolite. *Journal of Colloid and Interface Science* **348** (2), 585–590.

Ge, Y., Gao, T., Wang, C., Shah, Z. H., Lu, R. & Zhang, S. 2017 Highly efficient silica coated CuNi bimetallic nanocatalyst

from reverse microemulsion. *Journal of Colloid and Interface Science* **491**, 123–132.

Ho, Y. S. & McKay, G. 1999 Pseudo-second order model for sorption processes. *Process Biochemistry* **34** (5), 451–465.

Huang, X., Wang, Y., Liao, X. & Shi, B. 2010 Adsorptive recovery of Au^{3+} from aqueous solutions using bayberry tannin-immobilized mesoporous silica. *Journal of Hazardous Materials* **183** (1–3), 793–798.

Kim, Y.-H., Lee, B., Choo, K.-H. & Choi, S.-J. 2011 Selective adsorption of bisphenol A by organic–inorganic hybrid mesoporous silicas. *Microporous and Mesoporous Materials* **138** (1), 184–190.

Kuo, C.-Y. 2009 Comparison with as-grown and microwave modified carbon nanotubes to removal aqueous bisphenol A. *Desalination* **249** (3), 976–982.

Li, J., Zhan, Y., Lin, J., Jiang, A. & Xi, W. 2014 Removal of bisphenol A from aqueous solution using cetylpyridinium bromide (CPB)-modified natural zeolites as adsorbents. *Environmental Earth Sciences* **72** (10), 3969–3980.

Mall, I. D., Srivastava, V. C. & Agarwal, N. K. 2006 Removal of Orange-G and Methyl Violet dyes by adsorption onto bagasse fly ash–kinetic study and equilibrium isotherm analyses. *Dyes and Pigments* **69** (3), 210–223.

Manfo, F. P. T., Jubendradass, R., Nantia, E. A., Moundipa, P. F. & Mathur, P. P. 2014 Adverse effects of bisphenol A on male reproductive function. *Reviews of Environmental Contamination and Toxicology* **228**, 57–82.

Özacar, M. & Şengil, İ. A. 2003 Adsorption of reactive dyes on calcined alunite from aqueous solutions. *Journal of Hazardous Materials* **98** (1–3), 211–224.

Rochester, J. R. 2013 Bisphenol A and human health: a review of the literature. *Reproductive Toxicology* **42**, 132–155.

Shayesteh, H., Rahbar-Kelishami, A. & Norouzbeigi, R. 2016 Evaluation of natural and cationic surfactant modified pumice for Congo red removal in batch mode: kinetic, equilibrium, and thermodynamic studies. *Journal of Molecular Liquids* **221**, 1–11.

Singh, V. K. & Tiwari, P. N. 1997 Removal and recovery of chromium(VI) from industrial waste water. *Journal of Chemical Technology & Biotechnology* **69** (3), 376–382.

Sun, Y. J., Wang, H. W., Song, J. & Wang, J. X. 2010 Study on adsorption mechanism of ammonium ion by aged refuse. In: *Environmental Science and Information Application Technology (ESIAT), 2010 International Conference*, pp. 543–546.

Teng, M., Wang, H., Li, F. & Zhang, B. 2011 Thioether-functionalized mesoporous fiber membranes: sol–gel combined electrospun fabrication and their applications for Hg^{2+} removal. *Journal of Colloid and Interface Science* **355** (1), 23–28.

Tsai, W.-T., Hsu, H.-C., Su, T.-Y., Lin, K.-Y. & Lin, C.-M. 2006 Adsorption characteristics of bisphenol-A in aqueous solutions onto hydrophobic zeolite. *Journal of Colloid and Interface Science* **299** (2), 513–519.

Wu, S., Li, F., Wu, Y., Xu, R. & Li, G. 2010 Preparation of novel poly(vinyl alcohol)/SiO_2 composite nanofiber membranes with mesostructure and their application for removal of Cu^{2+} from waste water. *Chemical Communications* **46** (10), 1694–1696.

Yurtsever, M. & Sengil, I. A. 2009 Biosorption of Pb(II) ions by modified quebracho tannin resin. *Journal of Hazardous Materials* **163** (1), 58–64.

Zhang, L., Wang, W., Sun, S., Sun, Y., Gao, E. & Zhang, Z. 2014 Elimination of BPA endocrine disruptor by magnetic BiOBr@BiOBr@SiO_2@Fe_3O_4 photocatalyst. *Applied Catalysis B: Environmental* **148–149**, 164–169.

Zhao, D., Sun, J., Li, Q. & Stucky, G. D. 2000 Morphological control of highly ordered mesoporous silica SBA-15. *Chemistry of Materials* **12** (2), 275–279.

Zhou, H., Xu, Y., Tong, H., Liu, Y., Han, F., Yan, X. & Liu, S. 2013 Direct synthesis of surface molecularly imprinted polymers based on vinyl–SiO_2 nanospheres for recognition of bisphenol A. *Journal of Applied Polymer Science* **128** (6), 3846–3852.

First received 16 December 2016; accepted in revised form 24 April 2017. Available online 16 May 2017